DETERMINATION OF PHYSICAL PROPERTIES AND CALIBRATION OF DISCRETE ELEMENT SIMULATION PARAMETERS FOR YIMENG MOUNTAIN JUJUBES
/
沂蒙山红枣颗粒物性参数测定与离散元仿真参数标定

Fandi ZENG[1)], Hao ZHANG[2)], Yinzeng LIU[1)], Xiaofei CHENG[1)], Yuzhen DONG[1)], Zhihuan ZHAO[*1)], Haocheng LIU[1)]
[1)] Shandong Agriculture and Engineering University, College of Mechanical and Electronic Engineering, Jinan, China;
[2)] Shandong Agriculture and Engineering University, College of Food Science and Engineering, Jinan, China;
E-mail: zhaozhihuan@sdaeu.edu.cn
DOI: https://doi.org/10.35633/inmateh-79-89

Keywords: *Yimeng Mountain jujubes, Angle of repose, Box-Behnken test, The optimal parameter*

ABSTRACT
Accurate discrete element method (DEM) parameters are essential for simulating key operations in jujube postharvest processing, such as pneumatic cleaning during mechanical harvesting. The fundamental physical properties of Yimeng Mountain jujubes were systematically measured. A jujube particle template was constructed using the multi-sphere method, and the Hertz–Mindlin (no slip) contact model was adopted. The jujube simulation model was generated by filling the particle template with multiple spheres of different diameters. The static friction coefficient between jujubes ranged from 0.41 to 0.69, while that between jujubes and a steel plate ranged from 0.40 to 0.54. The rolling friction coefficient between jujubes ranged from 0.16 to 0.30, whereas that between jujubes and a steel plate ranged from 0.11 to 0.24. The coefficient of restitution between Yimeng Mountain jujubes, determined using a high-speed camera, ranged from 0.41 to 0.54, while that between jujubes and a steel plate ranged from 0.46 to 0.61. A Plackett–Burman screening design was conducted, and the results showed that the Poisson's ratio of jujube, the static friction coefficient between jujubes, and the static friction coefficient between jujubes and the steel plate were the three dominant factors. The steepest ascent method was then used to narrow the ranges of these significant parameters. Subsequently, a Box–Behnken design was employed to establish a quadratic regression model relating the angle of repose to the three significant factors. Using the experimentally measured angle of repose of 28.08° as the optimization target, the optimal simulation parameters were determined as follows: a Poisson's ratio of 0.32, a jujube–jujube static friction coefficient of 0.52, and a jujube–steel static friction coefficient of 0.47. The relative error between the simulated and experimentally measured angles of repose was 2.17%, further confirming the accuracy and reliability of the calibrated simulation parameters.

摘要
为沂蒙山红枣风选机械化采收等关键环节的仿真提供准确的离散元模型参数，本文通过物理试验精准测定红枣的物性参数. 本文对红枣颗粒模板进行单球形颗粒填充的方法,采用 Hertz-Mindlin (no slip)模型。红枣模拟模型是通过合并许多不同直径的球体而创建的使用 EDEM 软件的单个球形颗粒进行填充。采用斜面仪测得沂蒙山红枣之间的静摩擦系数为 0.41-0.69，沂蒙山红枣与钢板之间的静摩擦系数为 0.40-0.54。沂蒙山红枣之间的动摩擦系数为 0.16-0.30，沂蒙山红枣与钢板之间的动摩擦系数为 0.11-0.24。采用高速摄像机测得沂蒙山红枣与沂蒙山红枣的恢复系数为 0.41-0.54，沂蒙山红枣与钢板的碰撞恢复系数 0.46-0.61。开展 Plackett-Burman 试验筛选出对堆积角有显著影响的参数为：红枣泊松比、红枣-红枣静摩擦系数和红枣-钢静摩擦系数，进一步通过最陡爬坡试验确定显著性参数最优范围区间。通过 Box-Behnken 试验，建立堆积角与显著性参数的二阶回归模型，并以物理试验得到堆积角(28.08°)目标值进行优化求解，得到最优仿真参数：红枣泊松比为 0.32、红枣-红枣静摩擦系数为 0.52、红枣-钢静摩擦系数为 0.47。仿真堆积角与物理堆积角的相对误差为 2.17%。进一步验证了仿真试验和标定后仿真参数的真实性和可靠性。

INTRODUCTION
Yimeng Mountain jujube is a species in the genus Ziziphus, in the family Rhamnaceae. As a fruit-bearing tree, it provides substantial nutritional benefits and notable therapeutic qualities. A vital step in the production process is the collection of Yimeng Mountain jujubes. It has considerable seasonality and significant labour intensity. Jujube fruits during the ripening stage undergo natural desiccation on the tree before harvest. This technique optimally utilises solar and thermal resources *(Chu et al., 2012; Muqaddas et al., 2025)*. It can significantly enhance fruit quality. Winnowing machines are used in the Yimeng Mountain region for remove impurities during jujube harvesting.

Complex contact forces arise during the pneumatic separation process, both between jujube fruits and between the fruits and steel surfaces. These forces are difficult to measure directly using conventional experimental methods. Simulation can therefore be used to investigate the interaction mechanisms between jujube fruits and machinery during pneumatic separation, providing a basis for optimizing key equipment components and reducing fruit losses.

Research into basic agricultural materials has progressed significantly in recent years. These materials include soil *(Hao et al., 2025; Ji et al., 2025)*, straw *(Huang et al., 2025; Zhu et al., 2026)*, and seeds. The discrete element method has become an important approach for studying such problems. *Liu et al., (2025),* used the discrete element method to calibrate Cyperus esculentus seeds and determined the optimal parameter combination to overcome issues of irregular shape and uneven surface in high-speed precision seeding. *Ma et al., (2025),* investigated ruminant protein supplement pellets. They measured basic physical properties and contact characteristics, and built a discrete-element model. Using the angle of repose as an evaluation index in orthogonal tests, the optimal parameter combination was identified. *Gu et al., (2025),* calibrated the discrete element parameters of mustard leaf stems to visualise cutting and support numerical simulation; *Geng et al., (2026),* used the discrete element method to build a breakable 'Atlantic' potato seed model; *Chen et al., (2025),* established a paddy rice physical model with the multi-sphere (MS) approach. Validation tests were carried out using the cylinder-lifting method and the discharge mass-flow method. *Zheng et al., (2025),* focused on Fritillariae Thunbergii Bulbus (FTB). They developed a discrete element model of FTB using the Hertz-Mindlin bonding model. It took the maximum shear force as the evaluation index. The bond parameters in the model were then validated accordingly. *Yu et al., (*2025*),* developed DEM models of mallow and oats via the multi-sphere manual filling approach. These models were coupled with Fluent for gas-solid simulations. The study systematically analysed seed flow characteristics and seeding consistency in the distributor under varying inlet velocities and mass flow rates. *Li et al., (2026),* focused on dried safflower filaments. They calibrated the filament parameters by combining physical experiments with simulation tests. *Li et al., (2025)* selected Pizhou white garlic as the research object. Using EDEM software, a breakable, flexible discrete element model of garlic seed was built, and its bond parameters were calibrated. *Chen et al., (2024),* focused on optimising parameters for a pepper seeding device. A 3D seed model was constructed using reverse engineering. Key parameter ranges were then systematically determined. The discrete element method was used to study particle interactions and motion patterns. This approach helps reveal the mechanisms underlying particle–particle interactions and thus optimises key process parameters of equipment *(Ji et al., 2024*; *Zhou et al., 2023)*. Accurate discrete element method (DEM) parameters are essential for simulating key operations in jujube post-harvest processing, such as pneumatic cleaning during mechanical harvesting. However, research on accurate parameter calibration for jujube trees in Yimeng Mountain remains relatively limited.

This study accurately measured the intrinsic parameters of Yimeng Mountain jujubes through physical experiments. The free-fall principle and the inclined plane method were used. It determined the ranges of the coefficient of restitution, the static friction coefficient, and the rolling friction coefficient. The MATLAB software processed images of both the physical and simulated angles of repose. The edge contour was then fitted to obtain the angle of repose. The angle of repose from physical tests served as the evaluation index. Significant factors were screened using the Plackett-Burman design, followed by the steepest ascent and the Box-Behnken tests to determine the optimal simulation parameters. This study provides accurate discrete element model parameters for simulations of key processes, such as mechanised pneumatic harvesting of Yimeng Mountain jujubes.

MATERIALS AND METHODS

Determination of basic physical parameters

This study focuses on Yimeng Mountain jujubes as the research subject. Yimeng Mountain jujubes are bright red in colour, with thick flesh, small pits, a crisp texture when fresh, and a smooth, mellow taste when dried. One hundred jujubes were randomly selected, and the dimensions of each fruit were measured using a digital Vernier calliper with an accuracy of 0.02 mm. The three characteristic dimensions (length L, width W, and thickness T) were recorded. The volume of the Yimeng Mountain jujubes was measured using a graduated cylinder with a resolution of 1 mL. The moisture content was determined using the oven-drying method. The mean of the replicate measurements was taken as the final value. The experimental results are presented in Table 1.

Table 1

Basic physical properties of Yimeng Mountain jujubes

Parameter	Value
Mean dimensions (*L*×*W*×*T*)/mm × mm × mm	30.98×20.53×18.89
Mean mass (g)	4.64
Mean density (kg•m^3)	746
Mean moisture content (%)	18.58

Determination of the static friction coefficient

Jujubes were fixed to a plate using adhesive to form a jujube contact surface (Fig. 1a). A test jujube was placed on the surface, and the test plane was gradually inclined anticlockwise. When the jujube began to slide, the inclination was stopped and the corresponding angle displayed by the digital inclinometer was recorded. The static friction coefficient between jujubes was calculated using Eq. (1).

To determine the static friction coefficient between jujubes and steel, Yimeng Mountain jujubes were placed directly on the steel test surface, and the same procedure was followed (Fig. 1b). The static friction coefficient between jujubes ranged from 0.41 to 0.69, while that between jujubes and the steel plate ranged from 0.40 to 0.54.

$$\gamma = \tan\alpha \tag{1}$$

where, y is the static friction coefficient and α is the inclination angle of the test plane, (°).

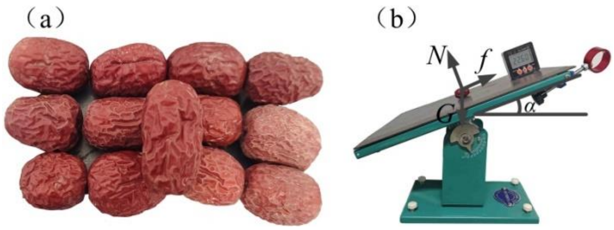

Fig. 1 - Measurement of the static friction coefficient
(a) Jujube contact surface; (b) Inclined-plane test setup

Determination of the rolling friction coefficient

The rolling friction coefficient was determined using a procedure similar to that used for the static friction coefficient. The inclination angle of the test plane was gradually increased until the jujube began to roll. The corresponding angle displayed by the digital inclinometer was then recorded. The rolling friction coefficient was calculated using Eq. (2). The rolling friction coefficient between jujubes ranged from 0.16 to 0.30, while that between jujubes and the steel plate ranged from 0.11 to 0.24.

$$\gamma_1 = \tan\alpha_1 \tag{2}$$

where, y_1 is the rolling friction coefficient and α_1 is the critical inclination angle at which rolling begins.

Determination of the coefficient of restitution

During the mechanical harvesting and cleaning of Yimeng Mountain jujubes, collisions occur both among the fruits and between the fruits and machine components, which may cause skin damage and internal injury. Therefore, the coefficient of restitution is an important contact parameter. The test setup for determining the coefficient of restitution is shown in Fig. 2 (*Hou et al., 2020*). Two impact surfaces were prepared: a steel plate and a plate formed by closely arranged Yimeng Mountain jujubes. Individual jujubes were released from rest from a fixed height of 400 mm and allowed to collide with the corresponding impact surface. After impact, the jujubes rebounded upward. The entire collision process was recorded using a high-speed camera, and the rebound characteristics were obtained through image post-processing.

The coefficient of restitution between Yimeng Mountain jujubes ranged from 0.41 to 0.54, while that between Yimeng Mountain jujubes and the steel plate ranged from 0.46 to 0.61.

$$e = \frac{v_2}{v_1} \tag{3}$$

where, v_1, and v_2 are the relative velocities before and after collision, respectively, m.s^{-1}.

The Yimeng Mountain jujubes were assumed to undergo free fall under the action of gravity. The normal velocity immediately before impact was calculated using the work–energy theorem.

$$v_1 = \sqrt{2gH} \tag{4}$$

The normal velocity immediately after impact was calculated as follows:

$$v_2 = \sqrt{2gh} \tag{5}$$

Therefore, the coefficient of restitution can be expressed as:

$$e = \sqrt{\frac{h}{H}} \tag{6}$$

where, H is the drop height before impact, mm; and h is the maximum rebound height after impact, mm.

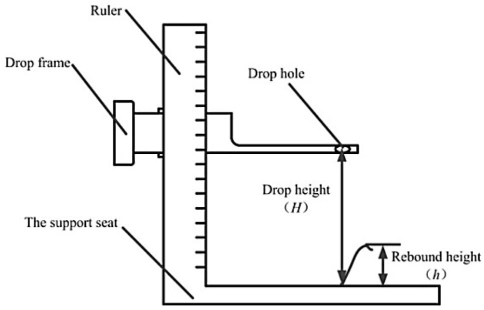

Fig. 2 - Schematic diagram of the test principle for coefficient of restitution

Angle of repose test

The angle of repose is defined as the angle between the slope of a granular pile and the horizontal plane. In the experiment, the inner diameters of the upper and lower openings of the funnel were 200 mm and 40 mm, respectively, and the vertical distance from the lower opening of the funnel to the horizontal test surface was 200 mm. A 200 g sample of Yimeng Mountain jujubes was placed in the funnel and allowed to fall freely onto the test surface, forming a conical pile. After the pile stabilized, the angle between the pile slope and the horizontal plane was taken as the experimentally measured angle of repose of the Yimeng Mountain jujubes. Images of the pile contour were captured using a camera and processed in MATLAB R2022b.

The images were imported using the imread function, converted to grayscale using rgb2gray, and then binarized using a fixed-threshold method. The region of interest was cropped, and the binary image was inverted. Internal holes in the target region were filled using the imfill function to improve the morphological integrity of the pile image. Edge detection was then performed to extract the contour of the jujube pile, and the coordinates of the boundary points were obtained. The first 50% of the boundary-point data were selected for coordinate transformation. A first-order polynomial was fitted to the transformed boundary points using the least-squares method. The angle of repose was subsequently calculated from the arctangent of the fitted slope. The fitting procedure is illustrated in Fig. 3. Each test was repeated 10 times, and the mean value was taken as the final result. The mean angle of repose of the Yimeng Mountain jujubes was 28.08°.

Fig. 3 - Image-processing procedure for determining the angle of repose
(a) Original image; (b) Morphological processing; (c) Contour extraction and fitting

Establishment of the simulation model

The fundamental physical properties of the Yimeng Mountain jujubes were determined through preliminary physical tests. A three-dimensional geometric model (particle template) was constructed in Creo based on the measured fruit dimensions. The model was exported in STEP format and imported into EDEM. The Hertz–Mindlin (no slip) contact model was adopted. To balance computational efficiency and model fidelity, the jujube particle model was constructed using the multi-sphere method. The particle template was filled with multiple spheres of different diameters in EDEM to generate the discrete element model of a jujube, as shown in Fig. 4a.

A simulation of the angle of repose test was then established using the same geometric dimensions as those employed in the physical test. A particle factory was positioned above the funnel to generate Yimeng Mountain jujube particles, which subsequently fell into the funnel under gravity.

The particle generation rate was 50 g/s, and a total particle mass of 200 g was generated. The particles continued to fall and accumulate on the test surface until the pile became stable. The angle between the pile slope and the horizontal test surface was taken as the simulated angle of repose. The particle size was kept constant throughout the simulation. The total simulation time was 4 s, the Rayleigh time step was set to 12%, the data-saving interval was 0.02 s, and the grid size was set to three times the minimum particle radius.

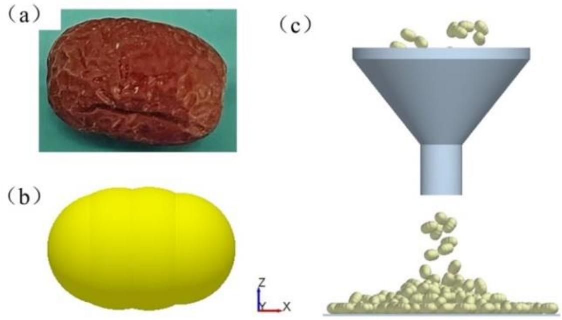

Fig. 4 - Simulation model for the angle of repose test
(a) Yimeng Mountain jujube; (b) Discrete element model of a jujube; (c) Simulation model of the angle of repose test

Simulation parameter calibration

Plackett-Burman test

The Design-Expert software was used for the Plackett-Burman test design. Test parameters were selected based on physical tests. The remaining simulation parameters were obtained from the relevant literature *(Du, 2022; Li, 2022; Shi et al., 2021; Zhou et al., 2022)*. Parameters exerting substantial influence on the response value were identified using the Plackett-Burman design. The principal elements that substantially affected the target response were identified. The parameters in Table 2 are encoded as +1 for maximum values and -1 for minimum values. At the end of each group of simulated trials, the angle of repose was measured using the same method employed in actual tests.

Table 2

Parameter ranges for the Plackett–Burman design

Code	Parameter	Low level (-1)	High level (+1)
X_1	Poisson's ratio of jujube	0.20	0.46
X_2	Shear modulus of jujube (MPa)	0.38	0.52
X_3	Jujube–jujube coefficient of restitution	0.41	0.54
X_4	Jujube–jujube static friction coefficient	0.41	0.69
X_5	Jujube–jujube rolling friction coefficient	0.16	0.30
X_6	Jujube–steel coefficient of restitution	0.46	0.61
X_7	Jujube–steel static friction coefficient	0.40	0.54
X_8	Jujube–steel rolling friction coefficient	0.11	0.24

Steepest ascent test

Based on the results of the Plackett–Burman design, a steepest ascent test was conducted for the significant parameters identified through the screening analysis. The relative error between the simulated and experimentally measured angles of repose was used as the evaluation index to determine the optimal ranges of the simulation parameters. The nonsignificant parameters were fixed at their mean values. The relative error between the simulated and experimentally measured angles of repose was calculated using Eq.(7).

$$\psi = \left| \frac{\theta - \theta_s}{\theta} \right| \times 100\% \tag{7}$$

where, ψ is the relative error between the simulated and experimentally measured angles of repose, %; θ_s is the simulated angle of repose, (°). θ is the experimentally measured angle of repose, (°).

Box - Behnken design

The optimal ranges of the significant factors were determined through the steepest ascent test and were subsequently used to define the factor levels. The angle of repose was selected as the response variable. A Box–Behnken design was then conducted for the significant parameters to determine the optimal parameter combination. The coded factor levels used in the simulation are presented in Table 3.

Table 3

Coded levels of the significant parameters

Coded level	Parameter		
	X_1	X_4	X_7
-1	*0.25*	*0.46*	*0.43*
0	*0.30*	*0.52*	*0.46*
+1	*0.36*	*0.57*	*0.48*

RESULTS

Analysis of the Plackett-Burman test results

The angle of repose of jujube particles on the steel plate was influenced by multiple factors. A Plackett-Burman test was therefore conducted to evaluate the significance of each factor. A total of 12 experimental runs were performed, and each run was repeated three times. The mean value was used for subsequent analysis. The experimental design and results are presented in Table 4, while the significance analysis of the Plackett–Burman factors is presented in Table 5. The screening results showed that X_1, X_4 and X_7 had significant effects on the angle of repose of the jujubes. Therefore, these three factors were selected for further analysis and optimization.

Table 4

Plackett–Burman design and simulation results

No.	Parameters								Angle of repose
	X_1	X_2	X_3	X_4	X_5	X_6	X_7	X_8	θ/(°)
1	1	-1	-1	-1	1	-1	1	1	30.28
2	-1	1	1	1	-1	-1	-1	1	23.46
3	1	1	-1	1	1	1	-1	-1	29.86
4	-1	-1	-1	-1	-1	-1	-1	-1	21.46
5	-1	-1	-1	1	-1	1	1	-1	32.54
6	1	-1	1	1	-1	1	1	1	36.44
7	-1	1	-1	1	1	-1	1	1	33.46
8	1	1	-1	-1	-1	1	-1	1	30.12
9	1	1	1	-1	-1	-1	1	-1	28.88
10	1	-1	1	1	1	-1	-1	-1	31.42
11	-1	-1	1	-1	1	1	-1	1	24.26
12	-1	1	1	-1	1	1	1	-1	32.46

Table 5

Significance analysis of the Plackett–Burman design

Parameters	Standardized effect	Sum of Squares	Contribution/(%)	Rank
X_1	3.23	31.23	14.49	3
X_2	0.31	0.28	0.13	6
X_3	-0.13	0.053	0.025	8
X_4	3.29	32.41	15.03	2
X_5	1.47	6.51	3.02	5
X_6	2.79	23.30	10.81	4
X_7	5.58	93.41	43.33	1
X_8	0.23	0.16	0.076	7

Analysis of the steepest ascent test results

The design and results of the steepest ascent test are presented in Table 6. As the Poisson's ratio of jujube and the jujube-jujube and jujube-steel static friction coefficients increased, the simulated angle of repose also increased. The relative error between the simulated and experimentally measured angles of repose first decreased and then increased. Run 3 produced the minimum relative error of 3.36%; therefore, its factor levels were selected as the centre point for the subsequent Box–Behnken design.

Table 6

Design and results of the steepest ascent test

No.	Parameters			Angle of repose (°)	Relative error (%)
	X_1	X_4	X_7		
1	0.20	0.41	0.40	21.34	24%
2	0.25	0.46	0.43	24.82	11.61%
3	0.30	0.52	0.46	27.06	3.36%
4	0.36	0.57	0.48	29.64	5.56%
5	0.41	0.63	0.51	32.44	15.53%
6	0.46	0.69	0.54	35.86	27.71%

Analysis of the Box–Behnken design results

The Box–Behnken experimental design and simulation results are presented in Table 7. Multiple regression analysis was performed on the simulation results, and a quadratic regression model for the simulated angle of repose was established as follows:

$$\begin{aligned}\theta = 27.43 - 0.72X_1 + 2.3X_4 + 1.33X_7 - 1.67X_1X_4 - 1.12X_1X_7 \\ -0.025X_4X_7 - 0.24X_1^2 + 2.05X_4^2 + 0.93X_7^2\end{aligned} \tag{8}$$

where, X_1 is the Poisson's ratio of jujube; X_4 is the jujube–jujube static friction coefficient; X_7 is the jujube–steel static friction coefficient.

The analysis of variance (ANOVA) for the quadratic regression model is presented in Table 8. X_1, X_4, X_7, X_1X_4, X_1X_7, X_4^2, X_7^2 had a significant impact on the angle of repose. The fitted angle of repose regression model had $P < 0.0001$. The lack-of fit term was P=0.6438 > 0.05. The model fit was good. The lack of fit was not significant. The coefficient of determination R^2 of the regression equation was 0.9898. The modified coefficient of determination R^2 was 0.9767, and the coefficient of variation *CV* was 1.33%. These results indicate that the regression model has good predictive ability and can be used to analyse and optimize the angle of repose.

Table 7

Box–Behnken design and simulation results

No.	Coding			Angle of repose (°)
	X_1	X_4	X_7	
1	0	0	0	26.88
2	1	0	1	27.34
3	0	-1	-1	26.66
4	0	0	0	28.04
5	1	-1	0	27.98
6	-1	-1	0	25.83
7	0	-1	1	29.66
8	0	0	0	27.36
9	0	0	0	27.54
10	-1	0	-1	26.68
11	0	1	-1	31.22
12	0	0	0	27.34
13	1	1	0	29.32
14	-1	0	1	31.26
15	1	0	-1	27.22
16	-1	1	0	33.85
17	0	1	1	34.12

Table 8

ANOVA for the quadratic regression model

Source of variance	Sum of squares	Degree of freedom	Mean square	*F*-value	*P*-value
Model	98.86	9	10.98	75.45	<0.0001**
X_1	4.15	1	4.15	28.49	0.0011**
X_4	42.23	1	42.23	290.05	<0.0001**
X_7	14.05	1	14.05	96.47	<0.0001**
$X_1 X_4$	11.16	1	11.16	76.62	<0.0001**
$X_1 X_7$	4.97	1	4.97	34.16	0.0006**
$X_4 X_7$	2.5E-003	1	2.5E-003	0.017	0.8994

Source of variance	Sum of squares	Degree of freedom	Mean square	*F*-value	*P*-value
X_1^2	0.24	1	0.24	1.65	0.2405
X_4^2	17.72	1	17.72	121.72	<0.0001**
X_7^2	3.65	1	3.65	25.09	0.0015**
Residual	1.02	7	0.15		
Lack of fit	0.32	3	0.11	0.61	0.6438
Pure error	0.7	4	0.17		
Cor total	99.88	16			

*Note: ** in Table 8 indicates that the impact is extremely significant(P<0.01), and * indicates that the impact is significant(P<0.05).*

Determination of the optimal parameters and experimental validation

The optimization objective was to minimize the difference between the simulated and experimentally measured angles of repose. The quadratic regression model was optimized using the experimentally measured angle of repose as the target value. Among the candidate solutions, the parameter combination closest to the mean values obtained from the physical measurements was selected. The optimal simulation parameters were determined as follows: Poisson's ratio, 0.32; jujube-jujube static friction coefficient, 0.52; and jujube-steel static friction coefficient, 0.47. To validate the calibrated discrete element parameters, the optimized parameter combination was used in EDEM simulations. Three repeated simulation tests were conducted, yielding angles of repose of 27.24°, 29.26°, and 29.58°. The mean simulated angle of repose was 28.69°, with a standard deviation of 1.04°. The relative error compared with the experimentally measured angle of repose of 28.08° was 2.17%. The close agreement between the simulated and experimental results further confirms the reliability and applicability of the calibrated simulation parameters.

DISCUSSION

In this study, the fundamental physical properties of Yimeng Mountain jujubes were systematically measured, and a three-dimensional geometric model incorporating their dimensional and morphological characteristics was established. A multi-sphere particle model was then developed in EDEM, in which the jujube geometry was represented by an assembly of spheres with different diameters. The coefficient of restitution, static friction coefficient, and rolling friction coefficient were determined using free-fall and inclined-plane tests. Images from both the physical and simulated angle-of-repose tests were processed in MATLAB, and the pile contours were fitted to determine the corresponding angles of repose. The experimentally measured angle of repose was used as the calibration target. Significant factors were identified using a Plackett–Burman design, followed by a steepest ascent test and Box–Behnken design to determine the optimal simulation parameters. Using the experimentally measured angle of repose as the optimization target, the calibrated parameters were determined as follows: Poisson's ratio of jujube, 0.32; jujube–jujube static friction coefficient, 0.52; and jujube–steel static friction coefficient, 0.47. The relative error between the simulated and experimentally measured angles of repose was 2.17%.

However, the calibration was conducted under ambient laboratory conditions, and the effects of variations in moisture content, temperature, and ripening stage on the contact parameters were not systematically investigated. Although the angle-of-repose test is widely used as a benchmark for evaluating bulk material behaviour, it represents only one quasi-static flow condition. Therefore, the calibrated parameters may not provide the same level of accuracy under highly dynamic conditions, such as high-velocity pneumatic conveying or rapid discharge. Validation using additional bulk-behaviour tests, such as shear-cell tests, hopper discharge tests, or direct shear tests, would further strengthen the general applicability of the calibrated parameter set. In addition, the present study focused primarily on jujube–jujube and jujube–steel contact parameters. Under actual harvesting and postharvest handling conditions, jujubes may also come into contact with materials such as rubber belts, plastic screens, and plant debris. Extending the calibration to these additional contact pairs would improve the practical applicability of the DEM model.

CONCLUSIONS

(1) The fundamental physical and contact parameters of Yimeng Mountain jujubes were determined through physical tests. The jujube–jujube static friction coefficient ranged from 0.41 to 0.69, while the jujube–steel static friction coefficient ranged from 0.40 to 0.54. The jujube–jujube rolling friction coefficient ranged from 0.16 to 0.30, whereas the jujube–steel rolling friction coefficient ranged from 0.11 to 0.24. The jujube–

jujube coefficient of restitution, determined using a high-speed camera, ranged from 0.41 to 0.54, while the jujube–steel coefficient of restitution ranged from 0.46 to 0.61.

(2) The measured physical and contact parameters were used to define the initial ranges of the DEM parameters. A Plackett–Burman design was conducted to screen the factors affecting the angle of repose. The Poisson's ratio of jujube, the jujube–jujube static friction coefficient, and the jujube–steel static friction coefficient were identified as the dominant factors. A steepest ascent test was then performed to further narrow the ranges of these parameters.

(3) A Box–Behnken design was subsequently employed to establish a quadratic regression model relating the angle of repose to the three dominant factors. Using the experimentally measured angle of repose of 28.08° as the optimization target, the optimal simulation parameters were determined as follows: Poisson's ratio of jujube, 0.32; jujube–jujube static friction coefficient, 0.52; and jujube–steel static friction coefficient, 0.47. The relative error between the simulated and experimentally measured angles of repose was 2.17%, indicating good agreement between the simulation and physical test results.

The calibrated parameters provide a basis for DEM simulations of key operations in the mechanical harvesting and postharvest handling of Yimeng Mountain jujubes, particularly pneumatic cleaning and separation processes, and can support further investigation of jujube motion and interaction behaviour during these operations. However, the present study adopted the Hertz–Mindlin (no slip) contact model, which is commonly used for dry, noncohesive particle systems in EDEM. Future work will consider more detailed contact and damage models, such as Bonding V2, to represent the skin and flesh of jujubes and to investigate fruit damage during harvesting. The effects of fruit morphology on DEM model accuracy will also be examined further.

ACKNOWLEDGEMENT

This project was funded by Shandong Agriculture and Engineering University Start-Up Fund for Talented Scholars (2024GCCZR-05). We also appreciate the work of the editors and the reviewers of the paper.

REFERENCES

[1] Chen, X. Y., Wang, X. Z., Bai, J., Fang, W. Q., Hong, T. Y., Zang, N. & Wang, G. L. (2024). Virtual parameter calibration of pod pepper seeds based on discrete element simulation. *Heliyon*, 10(11), e31686.

[2] Chen, Z. F., Che, G., Wan, L., Wang, H. C. & Zhang, K. (2025). Calibration and experimental validation of discrete element parameters for long-grain rice with different moisture contents based on angle of repose. *Agriculture*, 15(10), 1058.

[3] Chu, L., Wu, M.Y., Zhu, F.T., Zhao, Y., He, F.T., Ge, B.G. & Ma C. (2012). Industry Status and Development Proposal of Jujube in Xinjiang (新疆地区红枣产业现状及发展建议). *Academic Periodical of Farm Products Processing),* 4, 110–113.

[4] Du, X. (2022). Design and Experimental Research of Landing Red Jujube Harvesting Machinery (落地红枣收获机的设计与试验研究). Master's thesis. Xinjiang Agricultural University, Uumqi.

[5] Geng, H., Hu, J. M., Feng, Q., Sun, W., Yang, M., Wang, H. H., Qiao, W. H. & Wang, P. (2026). Calibration of V2 Discrete Element Model Parameters for Simulation of Atlantic Potato Slicing and Sorting. *Agriculture*, 16(4), 489.

[6] Gu, M., Shen, H. Y., Luo, W. W., Ling, J., Wang, B. K., Gu, F. W., Song, S. M., Pan, L. &Hu, Z. C. (2025). Calibration of Parameters for Leaf-Stem-Cutting Model of Tuber Mustard (Brassica juncea L.) Based on Discrete Element Method. *Agriculture*, 15(7), 773.

[7] Hao, B. E., Ma, X. J., Wang, L. X. & Tong, X. (2025). Discrete Element Method-Based Stratified Soil Modeling to Improve the Precision of Soil-Machine Interaction Simulations. *Agronomy*, 15(6), 1421.

[8] Hou, Z, F., Dai, N. Z., Chen, Z., Qiu, Y. & Zhang, X. W. (2020). Measurement and calibration of physical property parameters for Agropyron seeds in a discrete element simulation (冰草种子物性参数测定与离散元仿真参数标定). *Transactions of the Chinese Society of Agricultural Engineering*, 36(24), 46–54.

[9] Huang, H. N., Zhang, Y., Hou, G. Y., Su, B. H., Yin, H., Fu, Z. J., Zhuang, Y. F., Lv, Z. J., Tian, H. & Li, L. H. (2025). Establishment of Hollow Flexible Model with Two Types of Bonds and Calibration of the Contact Parameters for Wheat Straw. *Agriculture*, 15(15), 1686.

[10] Ji, C., Liu, W. R., Deng, Y. G., Wang, Y. Q., Chen, P. M. & Yan, B. (2025). Calibration of DEM Parameters and Microscopic Deformation Characteristics During Compression Process of Lateritic Soil with Different Moisture Contents. *Agriculture*, 15(14), 1548.

[11] Ji, J., Yu, L. H., Wu, X. M., Su, W., Xiao, Y. & Zhang, Z. (2024). Parameter Calibration of Discrete Element Simulation of Sorghum Seed for Wine Use (酒用高粱种子离散元仿真参数标定). *Journal of Agricultural Mechanization Research*, 46(09), 46–52.

[12] Li, H., Meng, Y. B., Qi, X. D., Wang, Y. J., Li, Y. Q. & Li, M. Y. (2025). Discrete Element Modelling Method and Parameter Calibration of Garlic Species Based on Bonding V2 Model (基于 Bonding V2 模型的蒜种离散元建模与参数标定). *Transactions of the chinese society for agricultural machinery*, 56(07), 150–157+169.

[13] Li, J. J. (2022). Design and experiment of picking up key components of self-propelled jujube harvester (自走式红枣收获机捡拾关键部件的设计与试验). Master's thesis. Tarim University, Tarim.

[14] Li, X. K., Xu, Y., Zhou, J. P., Wang, H. Y., Xu, X. & Zuo, J. W. (2026). Discrete elemental parameter calibration and experiments for mechanically harvested dried safflower filaments (机收干红花丝离散元参数标定与试验). *Transactions of the Chinese Society of Agricultural Engineering*, 42(04), 150–160.

[15] Liu, Z. Y., Yan, J. G., Liu, F. & Wang, L. J. (2025). Calibration and Testing of Discrete Element Simulation Parameters for the Presoaked Cyperus esculentus L. Rubber Interface Using EDEM. *Agronomy*, 15(10), 2440.

[16] Ma, G. Y., Zhang, S., Wang, H. F., Han, M. Y. & Sheng, S. Y. (2025). Calibration of contact parameters for ruminant protein supplement feed pellets based on the discrete element method. *INMATEH-Agricultural Engineering*, 77(3), 882–893.

[17] Muqaddas, Mengaya L., Ahmed M. M., Hamid S. M., Yanju X., Asim M. &Yunfeng P. (2025). Postharvest handling and storage strategies for preserving jujube (Ziziphus jujuba mill.) fruit quality: A review. *Foods*, 14(19), 3370.

[18] Shi, G. K., Li, J. B., Ding, L. P., Zhang, Z. Y., Ding, H. Z., Li, N. & Kan, Z. (2021). Calibration and tests for the discrete element simulation parameters of fallen jujube fruit. *Agriculture*, 12(1), 38.

[19] Yu, F., Wang, D. W., Wang, X. F., Wang, L., Hu, J. L., Chi, X. G. & Ji, M. (2025). Parameter Calibration and Experimentation of the Discrete Element Model for Mixed Seeds of Vetch (Vicia villosa) and Oat (Avena sativa) in a Pneumatic Seed Drilling System. *Applied Sciences*, 15(24), 13048.

[20] Zheng, H., Hu, Z. W., Xue, X. L., Ye, Y. X., Liu, T., Ren, N., Liu, F.Y. & Yu, G. H. (2025). Calibration and Experimental Validation of Discrete Element Parameters of Fritillariae Thunbergii Bulbus. *Applied Sciences*, 15(14), 7951.

[21] Zhou, J., Sun, W. T. & Liang, Z. A. (2023). Construction of Discrete Element Flexible Model for Jerusalem Artichoke Root-Tuber at Harvest Stage (收获期菊芋根-块茎离散元柔性模型研究). *Transactions of the chinese society for agricultural machinery*, 54(10), 124–132.

[22] Zhou, L., Li, J. B., Ding, L. P., Ding, H. Z. & Liang, J. P. (2022). Analysis and design of operating parameters of floor-standing jujube pickup device based on discrete element method. *Agriculture*, 12(11), 1904.

[23] Zhu, G.S., He, X. W., Wang, X. F., Shi J., Xing, J. F. & Wang, L. (2026). Physical properties and experimental study of cotton stalks from typical arid regions of southern Xinjiang based on DEM. *Agriculture*, 16(4), 427.